

# Self-calibration of Multiple Laser Planes for 3D Scene Reconstruction

Ryo Furukawa

Faculty of Information Sciences,  
Hiroshima City University, Japan  
ryo-f@cs.hiroshima-cu.ac.jp

Hiroshi Kawasaki

Faculty of Information Engineering,  
Saitama University, Japan  
kawasaki@cgv.ics.saitama-u.ac.jp

## Abstract

*Self-calibration is one of the most active issues concerning vision-based 3D measurements. However, in the case of the light sectioning method, there has been little research conducted on self-calibration techniques. In this paper, we study the problem of self-calibration for an active vision system which uses line lasers and a single camera. The problem can be defined as the estimation of multiple laser planes from the curves of laser reflections observed from a sequence of images captured by a single camera. The constraints of the problem can be obtained from observed intersection points between the curves. In this condition, the problem is formulated as simultaneous polynomial equations, in which the number of equations is larger than the number of variables. Approximated solutions of the equations can be computed by using Gröbner bases. By refining them using nonlinear optimization, the final result can be obtained. We developed an actual 3D measurement system using the proposed method, which consists of only a laser projector with two line lasers and a single camera. Users are just required to move the projector freely so that the projected lines sweep across the surface of the scene to get the 3D shape.*

## 1. Introduction

In the field of computer vision, calibration methods for two or more cameras have been studied extensively.

Especially, self-calibration methods for extrinsic parameters, in which 6-DOF pose parameters are estimated without a-priori information about the scene, have been studied by many researchers; these studies include passive systems [7] and active systems [15, 13] because of their usefulness and mathematical interest.

There are other kinds of calibrations. For example, in order to construct or use a range finder based on the light sectioning method, the relative position of the laser plane from the camera should be known. This may involve calibration to estimate the 3-DOF parameters of the plane. Ex-

amples of this kind of calibration are methods using objects of known shapes. Also, there are on-line calibration techniques using markers attached to fixed positions relative to the laser planes [9].

In the case of the light sectioning method, there has been little research on self-calibration. One of the reasons may be that it is not possible to form equations sufficient for solving the problem with a typical system formed by a camera and a line laser. This is in contrast to the case of stereo camera systems, in which much information is retrieved from a pair of images. Actually, redundant information obtained from the reflections of a line laser which can be used for self-calibration is very limited in comparison to stereo camera systems. One example to solve this problem is to fix the laser plane and the camera, and to scan the same scene multiple times using a mechanical platform[12].

Another approach is to use the information from multiple planes with the fixed scene to obtain more constraints, which is discussed in this paper. To achieve this, two methods can be considered: one is to project multiple laser planes from a projector which is composed of multiple line lasers, and the other is to capture a sequence of images by moving the laser projector. Either way, new equations can be formulated from the intersections of the detected curves of the laser reflections. If we can acquire a sufficient number of equations, the calibration problem may be solved.

In this paper, we study the problem of self-calibration by using a sufficient number of equations derived from the intersections of the multiple laser planes detected in a single image or a sequence of images. Formulation of this problem involves simultaneous polynomial equations with a large number of variables. These equations are difficult to solve. We show that, in some configurations, the problem is solvable and we provide a method to obtain numerical solutions. The solution is obtained by computing approximated solutions by using Gröbner bases and refining them using nonlinear optimization.

To test the proposed method, we developed an actual 3D measurement system, which consists of only a laser projector with two line lasers and a single camera. Because the

system is self-calibrated, users can start 3D scanning without any pre-calibration process and freely move the projector so that the projected lines sweep across the surface of the scene to get the 3D shape.

## 2. Related works

There are many existing commercial products which use the light sectioning method [5, 11]. With such systems that use the light sectioning method, the laser plane is fixed, or moved by precision mechanical devices. For these systems, laser plane calibration is required only once and precise calibration can be applied previously [19, 16].

On the other hand, in the case of a handheld 3D scanner, which is recently attracting wide attention because of its maneuverability and simplicity, the relationship between the laser plane and the camera position varies every time and must be calibrated on-line.

For example, Woo and Jung [2] have proposed an explicit calibration method; that is, they put a cubic frame in the field of view of the camera, and place an object inside this frame. Then, a laser emits a line beam to the object, and they can detect the bright point on the cube to estimate the pose of the beam plane and the 3D information. Bouguet and Perona [1] use shadows to calibrate the laser plane. They cast shadows on the known plane and estimate the parameters. Fisher et al. [8] have modified this idea. Furukawa and Kawasaki [9] have adopted a more active method. They place LED markers on the sensor itself and capture the markers with a single camera to estimate the laser plane. The abovementioned methods can solve the on-line laser plane calibration problems, however, they still have some drawbacks: for example, they require an object of a known shape [2, 1, 8] or markers [9] to be captured in the same frames for calibration.

Note that there are some handheld 3D scanners in which the laser plane projector and a camera are at a fixed position to each other [10, 18]. Such devices require laser plane calibration only once, therefore, the on-line laser plane calibration is not usually necessary.

There is another handheld 3D scanner which uses a laser plane only for the robust retrieval of correspondences for stereo vision system has been proposed [6]. With this system, they just use correspondences between two images for 3D reconstruction, and thus, the on-line laser plane calibration is not required.

As mentioned above, although many explicit calibration methods for the light sectioning method have been proposed, no self-calibration method has yet been proposed. This is mainly because a projected pattern on an unknown object from a single line-laser projector does not provide enough constraints for a solution. In this paper, we achieve self-calibration for the light sectioning method by using multiple line lasers. With our proposed method, all extra

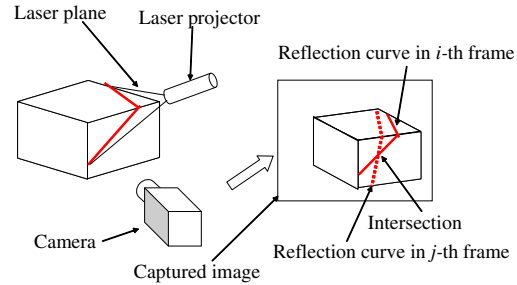


**Figure 1. Configuration of the active vision system.**

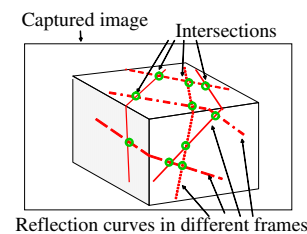


**Figure 2. Points of intersection of the reflection curves.**

devices for explicit calibration of laser plane can be eliminated; thus, the user can arbitrarily place a camera and freely move the laser projector without requiring known objects or attached markers to be captured in the frames.

## 3. Self-calibration for laser planes and camera

### 3.1. Problem definition

The minimum configuration of our target active vision system consists of a camera and a line laser projector, as shown in Figure 1. The intrinsic parameters of the camera such as the focal length are assumed to be known. Laser line projected from the projector is reflected at the surfaces of the scene and detected by the camera as curves in the images. We call these curves “reflection curves.”

A scanning process is performed by capturing a sequence of images with a fixed camera and moving the projector back and forth either manually or mechanically. Multiple reflection curves are obtained from the image sequence since they move in the image with the motion of the projector. The problem to solve is the estimation of the positions of the projected laser planes from the observed reflection curves. Once the positions of the laser planes become known, reconstruction of the 3D shapes of the scenes can be performed by triangulation.

By drawing all the reflection curves in different frames in a common image coordinates, those curves generally have intersections (Figure 2). Since the camera is fixed, an intersection of reflection curves corresponds to a 3D point on the scene. The point is on both of the two laser planes generating the curves. Therefore, we can acquire simultaneous equations using equations of laser planes and the observed coordinates of intersections as follows.

A plane which is not parallel to the  $z$  axis can be represented as  $ax + by + z + c = 0$  with  $a, b$ , and  $c$  as its parameters. Suppose that two planes whose indices are  $i$  and  $j$  and a surface have an intersection. The position of the point is  $(u_{i,j}, v_{i,j})$  in screen coordinates. Let the depth of the intersection from the camera be  $t_{i,j}$ , then the 3D point  $(u_{i,j}t_{i,j}, v_{i,j}t_{i,j}, -t_{i,j})$  is on the planes  $i$  and  $j$ . The  $z$  coordinate is negative since we assume the  $z$ -axis is directed backward from the camera. Representing the parameters of the plane  $i$  by  $a_i, b_i, c_i$ ,

$$\begin{aligned} a_i(u_{i,j}t_{i,j}) + b_i(v_{i,j}t_{i,j}) - t_{i,j} + c_i &= 0, \\ a_j(u_{i,j}t_{i,j}) + b_j(v_{i,j}t_{i,j}) - t_{i,j} + c_j &= 0. \end{aligned} \quad (1)$$

These equations can be obtained from all the intersections.

If the number of lines is  $n$  and the number of points of intersection is  $m$ , the total number of unknown parameters is  $3n + m$ , while the number of the constraints is  $2m$ . Obviously, the solutions are not fixed if the number of variables exceeds the number of equations. Therefore,  $3n + m \leq 2m$  (i.e.,  $3n \leq m$ ) is a necessary condition for this problem to have a finite number of solutions.

If we use multiple line lasers with fixed spatial relationships instead of a single line laser, additional constraints can be introduced between planes.

For example, suppose a laser projector which consists of two line lasers is aligned precisely at 90 degrees, as shown in Figure 3 (a). Using laser planes with different colors, these planes can be easily distinguished. Then, two different reflection curves, each of which corresponds to one of the laser planes, can be acquired from an image. From  $N$  images,  $2N$  reflection curves are observed. Simultaneous equations can be obtained in the same way as the case of the single line laser. Additional constraints are that two laser planes observed in the same image are perpendicular to each other. Indexing the laser planes at image  $k$  ( $0 \leq k \leq N - 1$ ) as the  $2k$ -th and  $(2k + 1)$ -th planes leads to this equation:

$$a_{2k}a_{2k+1} + b_{2k}b_{2k+1} + 1 = 0. \quad (2)$$

Using more laser planes attached to the projector, more constraints can be obtained.

In some conditions of the problem, the scaling factor of the scenes cannot be fixed. Typical examples of these conditions are the cases where a single laser plane or two laser planes are used. In these cases, an additional equation

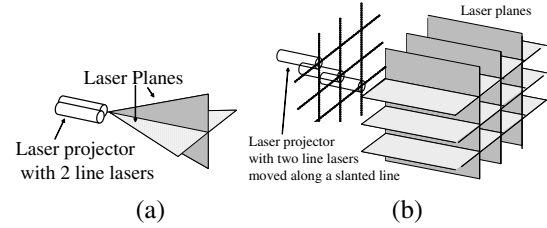


**Figure 3. A laser projector with two line lasers: (a) the configuration of the projector, (b) the grid pattern formed by moving the projector.**

should be used to avoid an ambiguity of the solutions. The equation is

$$t_{0,0} = 1. \quad (3)$$

An example of the opposite case is that, when multiple line lasers are placed in parallel, the scaling of the scene can be determined.

### 3.2. Examples of configurations

For the problem defined in Section 3.1 there are various system configurations in which the combination of two or more line lasers can be considered. These compositions are roughly classified into two methods.

The first method utilizes a sequence of measurements. In this case, the sequence of captured images with the laser projector moving and projecting the reflection curves onto the object, are used. By accumulating multiple captured images into one, intersections of projected laser curves are obtained to formulate the equations.

The other method is the case in which self-calibration can be performed from a single measurement. If enough line lasers are fixed to a device with their spatial relationships known, the position information of the device can be estimated from only one image.

#### 3.2.1 Solution using a sequence of measurements

In the case of configuring a laser projector with only a small number of line lasers, the configuration of two line lasers fixed at a certain angle gives a minimum configuration of line lasers in a projector in order for the problem to be solvable.

Let us consider the cross-plane laser projector mentioned in Section 3.1 (Figure 3 (a)). When we move the laser projector along a slanted line and capture 5 images as shown in Figure 3 (b), we can obtain a  $5 \times 5$  grid pattern and 25 intersections. Then, the number of planes is 10 and the unknown parameters for the planes are 30 and 25 for depth.

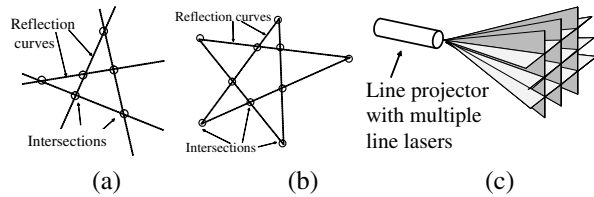


**Figure 4. Configurations of laser projectors with multiple line lasers.**

Thus, the number of total unknown parameters is 55. There are 50 equations for the intersections and 5 constraints of perpendicularity. With this configuration, uncertainty remains for the scaling factor; therefore, by adding the forms of equation (3), we have 56 equations. These simultaneous equations have finite solutions and can be solved. We will explain the details in Section 4.

Note that, a laser projector made of a single line laser is the simplest configuration; however, with this configuration, the simultaneous equation does not have finite solutions and cannot be solved. It is provable, but we omit the proof because of the limited number of pages. The fact that the single-line-laser configuration is not solvable also shows the importance of the constraints of perpendicularity, since they are the only difference between the single-line-laser configuration and the two-line-laser configuration.

### 3.2.2 Solution using a single measurement

In the case that four or more line lasers are attached to the projector and many intersections are observed at once, it is possible to perform self-calibration from a single image depending on the configurations.

For example, suppose that four line lasers are attached to a projector at known angles and six intersections are obtained from one image, as shown in Figure 4(a). By following the formulation described previously, 18 (i.e.,  $4 \times 3 + 6$ ) unknowns and 18 (i.e.,  $6 \times 2 + 6$ ) constraints are obtained. In this case, it is possible to perform a self-calibration from one view. If five line lasers are used as shown in Figure 4 (b), more constraints can be used and the solution can be estimated more precisely. In order to arrange many line lasers on the projector, aligning them to form a parallel or radiate grid is a practical method (Figure 4 (c)). If a parallel grid is adopted, it is also possible to determine scaling factor, making use of information on the intervals of the grid.

In these cases, it is easier to solve the problem by representing the relative pose between the projector and the camera as a maximum of 6-DOF parameters, rather than using the parameters of all the planes. Under the formulation using the relative pose as the parameters, the problem

becomes very similar to the the problem of self-calibration of the extrinsic parameters of a pair of cameras used in the stereo vision system. If all the laser planes share one point, the problem becomes equivalent to self-calibration between pinhole cameras, which can be solved by using the intersections of the reflection curves as correspondence points. The case where all the laser planes do not share one point is equivalent to the self-calibration between a pinhole camera and a generalized camera.

## 4. Range finder by projecting a cross-shaped pattern

### 4.1. System configuration

From the configurations described in the previous section, we developed a numerical solver for the case of two laser planes which intersect perpendicularly.

The reasons we adopted this setup are as follows: (1) as mentioned previously, it is the simplest solvable setup which requires the smallest number of line lasers, (2) distinction of the two laser planes can be easily achieved by using red and green line lasers, which are available as off-the-shelf products, and (3) mounting two planes perpendicularly is easy.

The actual scanning is performed as follows. First, we take five images while moving the projector, so that the reflection curves form a grid. Then an initial solution is obtained under the approximation of orthogonal projection (this process is described in Section 4.2). The solution is refined by a nonlinear optimization (this process is described in Section 4.4). The refined result of the self-calibration can be used for estimating the poses of the projector for all the frames in the image sequence and reconstructing the 3D scene.

### 4.2. Approximation for initial solution

In this section, the numerical solution for the problem described in Section 4.1 will be given. A brief description of the solution is as follows. First, the equation system which consists of 55 variables, 51 linear equations, and five quadratic equations is obtained from five images by approximating this problem using the assumption of orthogonal projection. This equation system can be converted to five quadratic equations with four variables by solving the linear equations. The converted simultaneous quadratic equations can be solved using Gröbner bases. Although the solution is for the approximated problem, the solution of the original problem can be obtained by performing nonlinear optimization using the obtained solution as initial parameters.

The reason for solving the approximated problem instead of the original one is that, since the original problem includes many (55) quadratic equations, the calculation of

Gröbner bases of the original equation set is intractable and the numerical solution cannot be obtained. By approximating the problem using the assumption of orthogonal projection, most of the equations become linear, resulting in only five quadratic equations with four variables. So, by reducing the scale of the problem using approximation, it becomes possible to apply the numerical solving method using Gröbner bases [3, 4].

Let the parameters of the vertical plane for the  $i$ -th image be  $(a_{v,i}, b_{v,i}, c_{v,i})$ . The same goes for the horizontal plane, whose parameters are  $(a_{h,i}, b_{h,i}, c_{h,i})$ . By limiting the intersections to those between the horizontal and vertical curves, a point can be indexed by two numbers: the image indices of the horizontal and vertical curves that form the intersection. Let the intersection of the vertical curve on the  $i$ -th image and the horizontal curve on the  $j$ -th image be expressed as intersection  $(i, j)$ . Also, let the depth of intersection  $(i, j)$  be  $t_{i,j}$ , and the image coordinates of intersection  $(i, j)$  be  $(u_{i,j}, v_{i,j})$ , using the screen coordinates of a normalized camera. From the forms of equation (1), we can obtain the simultaneous equations as follows:

$$\begin{aligned} a_{v,i}(u_{i,j}t_{i,j}) + b_{v,i}(v_{i,j}t_{i,j}) - t_{i,j} + c_{v,i} &= 0, \\ a_{h,j}(u_{i,j}t_{i,j}) + b_{h,j}(v_{i,j}t_{i,j}) - t_{i,j} + c_{h,j} &= 0, \end{aligned} \quad (4)$$

for  $1 \leq i, j \leq 5$ . The forms of equation (2) lead to

$$a_{v,i}a_{h,i} + b_{v,i}b_{h,i} + 1 = 0 \quad (5)$$

for  $1 \leq i \leq 5$ .

Now, we assume orthogonal projection. As already mentioned, using the configuration of two planes, the scaling of the object remains ambiguous. Therefore, we can assume that the distance to the object is a value near 1. Suppose the variation of  $t_{i,j}$  is sufficiently small and all  $t_{i,j}$  are near 1 (i.e., when the assumption of orthogonal projection can be applied), then, using the the forms of equation (4) can be transformed to

$$\begin{aligned} a_{v,i}(u_{i,j}) + b_{v,i}(v_{i,j}) - t_{i,j} + c_{v,i} &= 0, \\ a_{h,j}(u_{i,j}) + b_{h,j}(v_{i,j}) - t_{i,j} + c_{h,j} &= 0 \end{aligned} \quad (6)$$

for  $1 \leq i, j \leq 5$ . The equations are linear (note that  $u_{i,j}$  and  $v_{i,j}$  are constants), whereas the original equations are quadratic. Since there are 25 intersections, 50 linear equations of these forms are obtained.

The perpendicularity constraints between planes remain quadratic, which are expressed in the forms

$$a_{v,i}a_{h,i} + b_{v,i}b_{h,i} + 1 = 0 \quad (7)$$

for  $1 \leq i \leq 5$ . There are 5 equations of this form. As mentioned in Section 3.2.1, the perpendicularity constraints are important for the problem to be solvable. Since the perpendicularity constraints are quadratic of estimated parameters, it is difficult to convert the problem to simultaneous

linear equations which are easy to solve. Thus, we require a method to solve simultaneous quadratic equations.

Using orthogonal projection, the average of the depths to the scene remains ambiguous. To avoid the ambiguity, the equation (3) is added to the constraints.

### 4.3. Numerical solution

By the formulation described above, the number of variables is 55. The number of linear equations is 51. Using a matrix, these formulas are represented as follows:

$$\mathbf{M}\mathbf{x} = \mathbf{b} \quad (8)$$

where  $\mathbf{M}$  is a  $51 \times 55$  matrix whose elements are coefficients of equation (6), and  $\mathbf{x}$  is a 55-dimensional vector whose elements are variables of  $a_{h,j}$ ,  $b_{h,j}$ ,  $t_{i,j}$ , and  $\mathbf{b}$  is a 51-dimensional vector whose elements are 0, with the exception of one of them, which is 1 from equation (3).

This linear equation is under-constrained. By applying SVD (singular value decomposition) to the matrix, we can obtain a 5D linear space of  $\mathbf{x}$  in which equation (8) is approximately fulfilled. This can be done by the following steps. By applying SVD to  $\mathbf{M}$ , the equation becomes as follows:

$$\mathbf{U}\mathbf{\Sigma}\mathbf{V}\mathbf{x} = \mathbf{b}. \quad (9)$$

where  $\mathbf{U}$  is a  $51 \times 51$  matrix and  $\mathbf{V}$  is a  $55 \times 55$  matrix. Now, let the matrix formed by the upper 50 rows of  $\mathbf{V}$  be  $\mathbf{V}_1$ , the the matrix formed by the lower 5 rows of  $\mathbf{V}$  be  $\mathbf{V}_2$ , and  $\mathbf{U}_1$  be the upper right,  $50 \times 50$  submatrix of  $\mathbf{U}$ . Assuming that the rank of  $\mathbf{M}$  is 50 or 51, then the approximated solution space of the equation can be expressed as

$$\mathbf{x} = \mathbf{V}_1^t \mathbf{\Sigma}^{-1} \mathbf{U}_1^t \mathbf{b} + \mathbf{V}_2^t \mathbf{f} \quad (10)$$

where  $\mathbf{f} = (f_0, f_1, f_2, f_3, f_4)$  is an arbitrary 5D vector. The assumption of  $\mathbf{M}$  having a rank of 50 or higher will be empirically confirmed in Section 5.

By substituting the elements of  $\mathbf{x}$  in the equation (7) using (10), five simultaneous quadratic equations with variables  $f_0, f_1, f_2, f_3$  and  $f_4$  are obtained. We solve these equations numerically using Gröbner bases.

The group of a polynomial equation can be treated as an ideal in the field of commutative algebra. The ideal which represents simultaneous polynomial equations can be generated by finite bases in the same way that vector space is spanned by basis vectors. Bases with a special property which generate an ideal are called Gröbner bases.

The method to obtain the numerical solution of simultaneous polynomial equations using Gröbner bases is described in [3, 4] and [17]. More specifically, Gröbner bases are obtained from the original equations; then, a matrix called the "action matrix" corresponding to the target variable is calculated. The eigenvalues of this action matrix constitute the solutions.

From the solver of simultaneous quadratic equations based on Gröbner bases, multiple complex solutions of  $(f_0, f_1, f_2, f_3, f_4)$  are obtained. From these solutions, we select solutions which are near to the real solutions. Typically, we obtain several (nearly) real solutions of  $(f_0, f_1, f_2, f_3, f_4)$ . Solutions of  $\mathbf{x}$  are obtained from the solutions of  $(f_0, f_1, f_2, f_3, f_4)$ .

#### 4.4. Refinement of the solution

The numerical solution estimated in the previous section is a solution of the approximated problem. Therefore, the solution of the original problem is estimated by improving the obtained solution by nonlinear optimization. We can use the errors of equation (6),(7) and (3) to form the objective function to be optimized. However, the forms of equation (6) are "soft" constraints (i.e., they may not be strictly fulfilled) since they use observed values, whereas the forms of equation (7) are "hard" constraints (i.e., they should be strictly fulfilled). Moreover, it is desirable that the objective function represents the observation errors in screen space as bundle adjustments. Therefore, we take another approach.

The poses of the projector which projects two planes are used as parameters of the objective function. The degree of freedom of such a pose is 5. The actual parameters of a pose are the rotation parameters of roll, pitch, and yaw, and distances from the origin to each of the two planes. By expressing the direction of the two planes by the rotation, the forms of equation (7) are strictly fulfilled.

The line of intersection of the vertical plane of the  $i$ -th image and the horizontal plane of the  $j$ -th image is calculated, and is projected in the image. Representing the projected line as  $l_{i,j}$ , the intersection  $(i, j)$  should be on  $l_{i,j}$ . Therefore, the objective function is calculated as the sum of the squared distances between intersections  $(i, j)$  and the lines  $l_{i,j}$  for all  $i, j$ . In this formulation, the depths are not parameters. The depths are estimated from the poses as the depth of the point on  $l_{i,j}$  nearest to intersection  $(i, j)$ . Furthermore, to fix the scale, the squared error of equality 1 is added to the objective function. Minimization of the objective function is performed using the Levenberg-Marquardt method.

### 5. Experiments

In order to confirm the validity of the self-calibration technique described in Section 4, some experiments were conducted with simulated and actual data.

We used two types data for simulation. One generated precise, numerically synthesized data, fulfilling the equations (4) and (5) with a precision on the order of  $10^{-16}$ . The other data was generated by a CG renderer. Using this renderer, we could obtain data of an arbitrary 3D model. Actual data was obtained by the specially configured device.

#### 5.1. Numerically synthesized data

The numerically synthesized test data is generated as follows. Five poses of the projector are generated. They are similar but varied randomly. From the poses, 25 intersection points are calculated, whose depths are varied randomly. The area of the bounding box of the points was from -0.098 to 0.048 for  $x$ , from -0.102 to 0.066 for  $y$ , and from -1.029 to 0.97 for  $z$ . Then, the points are projected onto the screen coordinates, using both orthogonal projection and perspective projection. The projected coordinates are denoted as  $(u_{i,j}^*, v_{i,j}^*)$ (orthogonal) and  $(u_{i,j}, v_{i,j})$ (perspective).

To formulate a problem with simultaneous equations, the Jacobian of the equations should be full rank; otherwise, the equations may have infinite number of solutions instead of finite number of solutions. To verify that the problem has finite solutions, we calculated the singular values of the Jacobian. From equations (3)(4) and (5), the Jacobian was calculated symbolically, and the variables of the Jacobian were substituted by the synthesized data. The maximum singular value of the Jacobian was 2.8 and the minimum singular value was 0.0002892. This calculation was performed with Mathematica. Thus, it was full rank. This means that, in general, the self-calibration problem of this configuration has finite solutions.

As described in Section 4.3, we assumed that the rank of matrix  $\mathbf{M}$  is either 50 or 51. For the simulated data, the maximum singular value in the double-precision floating-point format was 2.6521308491146147. The 50th singular value was 0.0019077525332519675 and the 51st was 0.00018489169719173784. To perform SVD, the LAPACK numerical library [14] was used. Considering the precision, we can say that the rank of  $\mathbf{M}$  is either 50 or 51.

Next, we tested the numerical solver described in Section 4.3 with the synthesized data. We applied the solver to the data and obtained the parameters of all the laser planes and the depths of the intersection points. Since the scaling factor cannot be determined, we scaled the solution by the true value of  $t_{0,0}$  so that the solution could be compared.

The solution from the data of the orthogonal projection should be the same as the true values. In fact, for the solution calculated from  $(u_{i,j}^*, v_{i,j}^*)$ , the RMS (root of mean squared) error of  $t_{i,j}$  ( $1 \leq i, j \leq 5$ ) was  $4.70 \times 10^{-6}$ . So, the solver worked correctly. The solution obtained from  $(u_{i,j}, v_{i,j})$  was deviated from the true values because of the approximation described in Section 4.2. The deviation is shown in Figure 5.

Then, we tested the refinement of the solution described in Section 4.4. We applied the refinement algorithm to the solution obtained from the data of perspective projection. Figures 6 (a) and (b) show the result. Comparing the result with figure 5, it is confirmed that the solution was improved, although there remain errors.

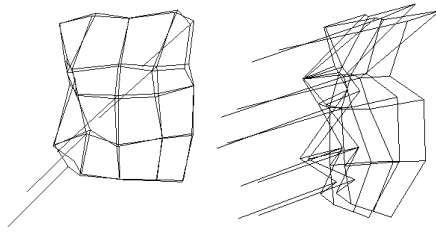


**Figure 5. The solution of the approximated problem with the true values. (The lines drawn from five of the grid points show the directions from the point to the projector.)**

We also tested the refinement process with noised data. To the synthesized data, we added uniform noise distributed between -0.001 and 0.001 to the constants  $u_{i,j}$  and  $v_{i,j}$ . Generating ten sets of data with this method, the refinement was performed for each of the data. The results are shown in figures 6 (c) and (d).

### 5.2. CG-synthesized data

Next, we tested the method with the data generated by CG rendering. Figure 7 shows the example of a scene composed of a cube and a plane. In the figure, (a) describes all the patterns which is detected by the camera. The angle of sight of the height of the image was 10 degrees. The borders of the black and white pattern on the scene indicates where the laser curves should be observed. Five of the intersections marked with crosses are the intersections where the laser planes intersect at right angles. Figure 7 (b) shows the 3D wireframe of the true shape of the grid in the scene. Figure 7 (c) is the result of the solution using approximation, and (d) is the result of the refinement. These results are shown with the true shape of the grid. With this example, the refinement worked very well, so that the refined solution and the true values became very close.

### 5.3. Actual system

We built an actual active vision system based on the method described in section 3. The laser projector consists of two line lasers fixed at 90 degrees; one of them is red and the other is green. The video sequence is captured by DV camera and intersection points are obtained by detecting laser-curves on each frame.

For experiments, we scanned a plastic object with a sinusoidal curve, as shown in Figure 8(a). Figure 8 (b) shows the sample input images. The estimated 3D points and shapes are shown in Figures 8(c) - (g). With those results, we can confirm that the shape is successfully recovered with our proposed method.

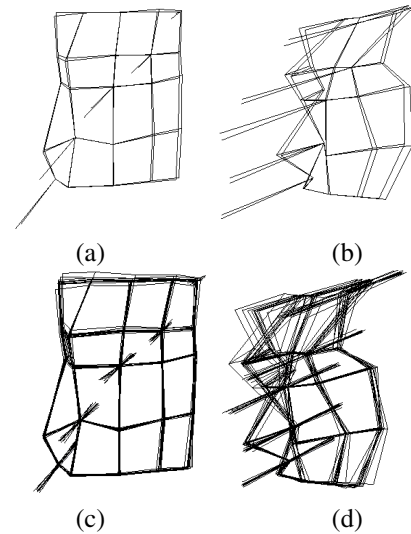


**Figure 6. The refined solution: (a),(b) the solution (shown with the true values), (c),(d) the solutions with noised data. (The lines drawn from five of the grid points show the directions from the point to the projector.)**

## 6. Conclusion

In this paper, we proposed a self-calibration method of multiple laser planes, which are parts of a laser sectioning method. The algorithm is as follows: first, we capture an image sequence while moving a laser projector back and forth; second, we obtain the intersections of the projected laser curves from the image sequence; and, finally, we solve the simultaneous equations which are formulated from the intersections.

We presented, as the simplest solvable configuration, an implementation with a configuration of two line lasers at fixed angles (90 degrees). With this device, an enough number of constraint equations to solve the problem are derived from 5 images. The equations are difficult to solve, since the size of the problem is large and it is difficult to convert them into linear equations. We proposed a method to solve the equations, in which approximated solutions are obtained by using Gröbner bases and are refined by nonlinear optimization. Using the proposed method, we can create a 3D measurement system which consists of only a laser projector with two line lasers and a single camera.

In order to verify the reliability and effectiveness of the proposed method, we conducted a simulation for evaluation. We also implemented an actual 3D scanner and performed several experiments with the system. The results of our experiments confirmed the effectiveness of the proposed system.

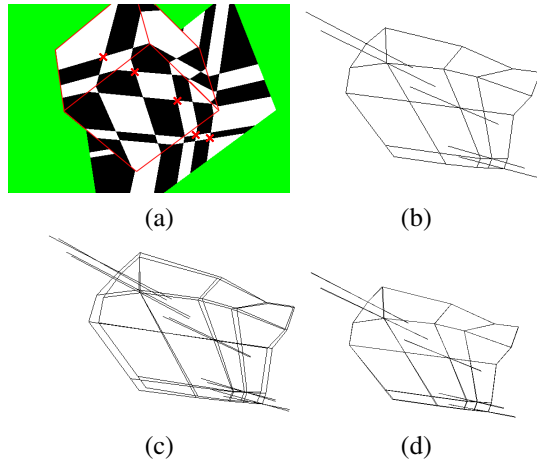


**Figure 7. Results of the data generated by CG : (a) the detected pattern, (b) the true 3D shape of the grid, (c) the result of the approximated problem (with the true shape), and (d) the result of the refined solution (with the true shape).**

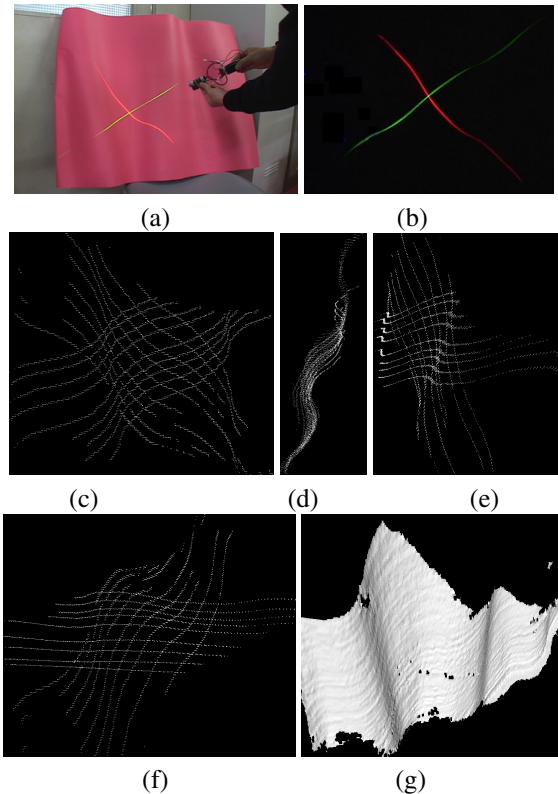


**Figure 8. Scanning of a sinusoidal curved object: (a) the target object and capturing scene, (b) projected laser-lines and (c),(d),(e) (f) and (g) result of 3D estimation.**

## References

- [1] J. Y. Bouguet and P. Perona. 3D photography on your desk. In *Int. Conf. Computer Vision*, pages 129–149, 1998.
- [2] C. W. Chu, S. Hwang, and S. K. Jung. Calibration-free approach to 3D reconstruction using light stripe projections on a cube frame. In *Third Int. Conf. on 3DIM*, pages 13–19, 2001.
- [3] D. A. Cox, J. B. Little, and D. O’Shea. *Ideals, Varieties, and Algorithms*. Springer-Verlag, NY, 2nd edition, 1996. 536 pages.
- [4] D. A. Cox, J. B. Little, and D. O’Shea. *Using Algebraic Geometry*, volume 185 of *Graduate Texts in Mathematics*. Springer-Verlag, NY, 1998. 499 pages.
- [5] Cyberware. Desktop 3D scanner. In <http://www.cyberware.com/>.
- [6] J. Davis and X. Chen. A laser range scanner designed for minimum calibration complexity. In *Int. Conf. on 3DIM2001*, pages 91–98, 2001.
- [7] O. Faugeras. *Three-Dimensional Computer Vision - A Geometric Viewpoint*. Artificial intelligence. M.I.T. Press Cambridge, MA, 1993.
- [8] R. B. Fisher, A. P. Ashbrook, C. Robertson, and N. Werghi. A low-cost range finder using a visually located, structured light source. In *Second Int. Conf. on 3DIM*, pages 24–33, 1999.
- [9] R. Furukawa and H. Kawasaki. Interactive shape acquisition using marker attached laser projector. In *Int. Conf. on 3DIM2003*, pages 491–498, 2003.
- [10] P. Hebert. A self-referenced hand-held range sensor. In *Int. Conf. on 3DIM2001*, pages 5–12, June 2001.
- [11] L. D. Inc. 3D laser scanners. In <http://www.laserdesign.com/>.
- [12] O. Jokinen. Self-calibration of a light striping system by matching multiple 3-d profile maps. In *2nd International Conference on 3D Digital Imaging and Modeling (3DIM ’99)*, pages 180–190, 1999.
- [13] H. Kawasaki and R. Furukawa. Uncalibrated multiple image stereo system with arbitrarily movable camera and projector for wide range scanning. In *Int. Conf. on 3DIM2005*, pages 302–309, June 2005.
- [14] lapack@cs.utk.edu. Lapack — linear algebra package. In <http://www.netlib.org/lapack/>.
- [15] Y. F. Li and R. S. Lu. Uncalibrated euclidean 3D reconstruction using an active vision system. *IEEE Transactions on Robotics and Automation*, 20(1):15–25, 2004.
- [16] A. M. McIvor. Nonlinear calibration of a laser stripe profiler. *Optical Engineering*, 41:205–212, Jan. 2002.
- [17] H. Stewenius. *Grobner Basis Methods for Minimal Problems in Computer Vision*. PhD thesis, Lund Institute of Technology, 2005.
- [18] K. H. Strobl, W. Sepp, E. Wahl, T. Bodenmueller, M. Suppa, J. F. Seara, , and G. Hirzinger. The dlr multisensory hand-guided device: The laser stripe profiler. In *ICRA2004*, pages 1927–1932, apr 2004.
- [19] G. B. Wolfgang Stocher. Automated simultaneous calibration of a multi-view laser stripe profiler. In *ICRA2005*, 2005.